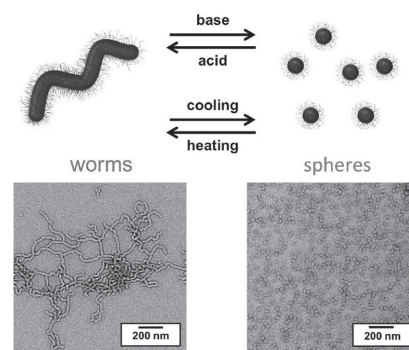# Characterization of Diblock Copolymer Order–Order Transitions in Semidilute Aqueous Solution Using Fluorescence Correlation Spectroscopy

Christopher G. Clarkson, Joseph R. Lovett, Jeppe Madsen, Steven P. Armes,* Mark Geoghegan*

The temperature and pH-dependent diffusion of poly(glycerol monomethacrylate)-*block*-poly(2-hydroxypropyl methacrylate) nanoparticles prepared via polymerization-induced self-assembly in water is characterized using fluorescence correlation spectroscopy (FCS). Lowering the solution temperature or raising the solution pH induces a worm-to-sphere transition and hence an increase in diffusion coefficient by a factor of between four and eight. FCS enables morphological transitions to be monitored at relatively high copolymer concentrations (10% w/w) compared to those required for dynamic light scattering (0.1% w/w). This is important because such transitions are reversible at the former concentration, whereas they are irreversible at the latter. Furthermore, the FCS data suggest that the thermal transition takes place over a very narrow temperature range (less than 2 °C). These results demonstrate the application of FCS to characterize order–order transitions, as opposed to order–disorder transitions.

1. Introduction

It is well known that amphiphilic diblock copolymers can self-assemble in aqueous solution to form ordered micellar gels at relatively high concentrations.[1,2] Judicious choice of the copolymer allows the design of hydrogels that are responsive to temperature[3,4] or pH.[5–8] However, it is relatively unusual for such a copolymer to respond to both temperature and pH.

In principle, biocompatible block copolymer gels can be used as a long-term cell storage medium.[9] One promising candidate for such applications is a diblock copolymer comprising poly(glycerol monomethacrylate) (PGMA) and poly(2-hydroxypropyl methacrylate) (PHPMA), which are conveniently prepared via polymerization-induced self-assembly[9–13] using reversible addition-fragmentation chain transfer (RAFT) aqueous dispersion polymerization.[14–16] This versatile approach has enabled spherical, worm-like or vesicular copolymer morphologies to be generated in concentrated solution.[11,17–26] Such a nonionic PGMA-PHPMA diblock copolymer exhibits a thermoreversible

C. G. Clarkson, Prof. M. Geoghegan
Department of Physics and Astronomy
University of Sheffield
Hounsfield Road, Sheffield S3 7RH, UK
E-mail: mark.geoghegan@sheffield.ac.uk
J. R. Lovett, Dr. J. Madsen, Prof. S. P. Armes
Department of Chemistry
University of Sheffield
Brook Hill, Sheffield S3 7HF, UK
E-mail: s.p.armes@sheffield.ac.uk

Characterization of Diblock Copolymer Order–Order Transitions in Semidilute Aqueous Solution Using Fluorescence . . .

Macromolecular
Rapid Communications

www.mrc-journal.de

order–order transition from worms to spheres upon cooling from 20 to 4 °C, as a result of greater hydration of the core-forming PHPMA block at the lower temperature (Figure 1a,c,d).[9] However, very recently it was reported that end-group chemistry can be exploited in order to introduce pH-dependent behavior in addition to such thermoresponsive behavior (Figure 1b).[27]

More specifically, a carboxylic acid-based RAFT chain transfer agent (CTA) was utilized in the preparation of the hydrophilic PGMA block in order to confer pH-dependent behavior on the nonionic diblock copolymer chains.[27] Thus raising the solution pH above the pK$_a$ of 4.7 causes ionization of the terminal carboxylic acid group and hence introduces anionic charge, which in turn leads to a pH-induced worm-to-sphere transition (Figure 2).[27]

Spherical diblock copolymer nanoparticles produce a low-viscosity, free-flowing solution that can be readily sterilized via ultrafiltration, which has important biomedical implications.[9] Aqueous dispersions of worms are much more viscous, with free-standing gels being formed in semidilute aqueous solution as a result of multiple inter-worm contacts. Below the critical gelation concentration, PGMA-PHPMA worms can diffuse freely in solution albeit rather more slowly than the (many) spheres from which they are formed. Thus monitoring the rate of diffusion is a potentially powerful technique for characterizing the worm-to-sphere transition. In particular, fluorescence correlation spectroscopy (FCS) is an excellent tool for measuring diffusion coefficients, because it allows access to a wide range of time scales.[28–32] FCS makes use of a confocal experimental setup to achieve high spatial and temporal resolution. Unlike confocal microscopy, FCS only requires a relatively low fluorophore concentration. This is because the latter is sensitive to fluctuations in fluorescence intensity and hence requires far fewer dye labels to diffuse through the confocal volume for analysis. In general, the concentration of fluorescently tagged molecules should be of the order of 10 µmol m^{-3}, such that there is on average only one dye label within the detection volume at any given time. It is well established that FCS is an ideal

tool for measuring conformational transitions[33,34] and for studying the behavior of polymeric micelles.[35,36] In the present study, the rate of diffusion is sensitive to the copolymer morphology, which makes this technique well suited for examining the diffusion of rhodamine-labeled diblock copolymer worms/spheres as a function of both pH and temperature.

2. Experimental Section

A PGMA$_{43}$ macro-CTA containing a terminal carboxylic acid group was prepared via RAFT solution polymerization in ethanol using 4-cyano-4-(2-phenylethane sulfanylthiocarbonyl)
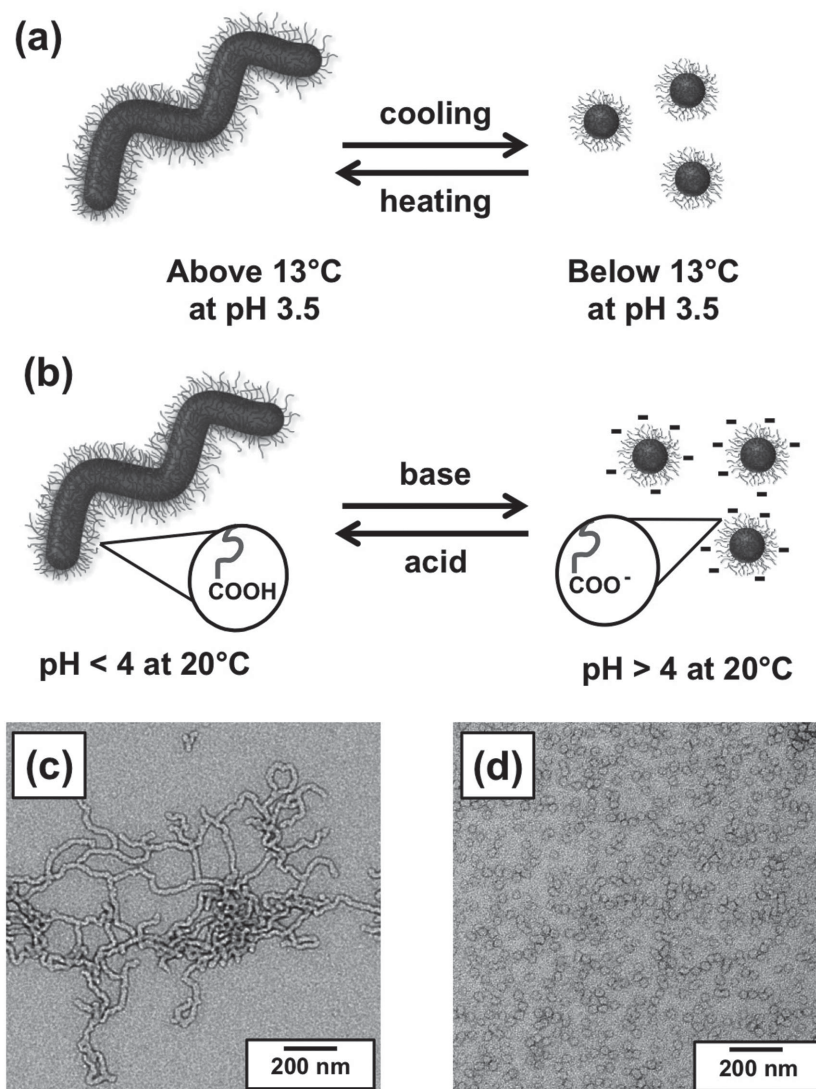

Figure 1. Top) Schematic cartoon of the reversible worm-to-sphere transition that occurs when PGMA-PHPMA diblock copolymer worms are subjected to: a) cooling below 13 °C at pH 3.5 or b) a pH switch via addition of base at 20 °C. Bottom) Transmission electron microscopy images obtained for PGMA$_{43}$-*block*-P(HPMA$_{119}$-*co*-GlyMA$_1$) copolymer diluted to 0.1 w/w % in acidic aqueous solution (pH 3.5) at c) 20 °C and d) 5 °C.
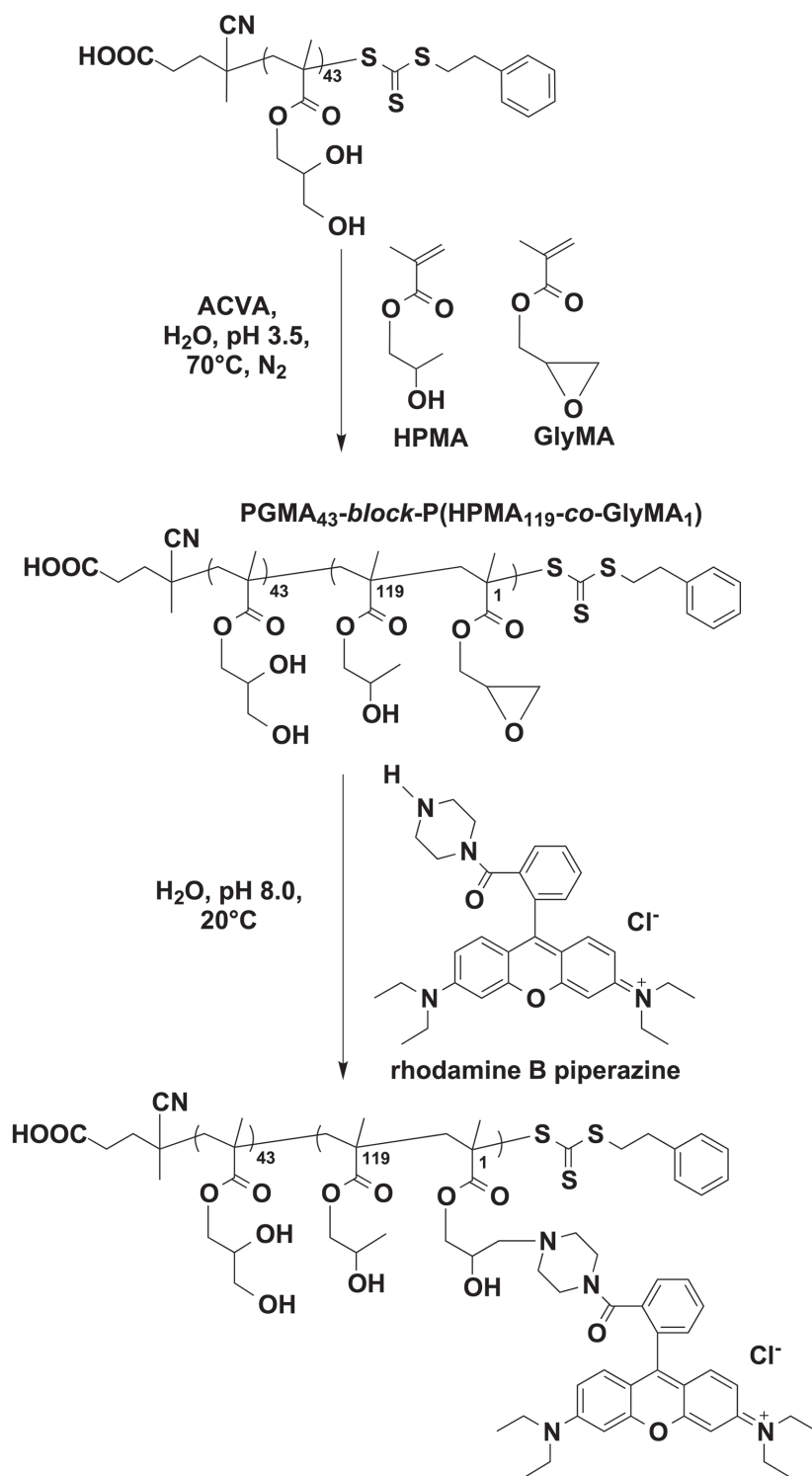
Figure 2. Chain extension of a carboxylic acid-terminated PGMA$_{43}$ macro-CTA via RAFT aqueous dispersion copolymerization of HPMA with GlyMA to form a well-defined PGMA$_{43}$-*block*-P(HPMA$_{119}$-*co*-GlyMA$_1$) worm gel at pH 3.5.

GlyMA (targeting approximately one epoxy group per copolymer chain) at 70 °C at approximately pH 3.5. ^{1}H NMR studies confirmed that a very high HPMA conversion (>99%) was achieved at 10% solids, while gel permeation chromatography analysis (N,N′-dimethylformamide eluent) indicated a relatively high blocking efficiency (>90%) and a relatively low copolymer dispersity (M_w/M_n = 1.20). The resulting HOOC-PGMA$_{43}$-*block*-P(HPMA$_{119}$-*co*-GlyMA$_1$) worms formed a soft, transparent free-standing gel at 10% w/w in mildly acidic solution (pH < 4). Rhodamine B (RhB) was used as a fluorescent probe; this dye label was incorporated into the hydrophobic P(HPMA$_{119}$-*co*-GlyMA$_1$) core-forming block by reacting a sub-stoichiometric amount of rhodamine B piperazine with the pendant epoxy groups (dye/epoxy molar ratio = 0.25). Using free rhodamine B piperazine dye to construct a Beer–Lambert linear calibration plot, visible absorption spectroscopy studies of the dissolved fluorescently labeled diblock copolymer in methanol prior to dilution for FCS measurements suggested that 18% (compared to a target of 20%) of the copolymer chains were fluorescently labeled (see Figure S1 in the Supporting Information). Furthermore, high-performance liquid chromatography analysis of the copolymer immediately after dye conjugation confirmed negligible contamination by the free dye (see Figure S2 in the Supporting Information). The dye content was sufficiently low that it had a negligible effect on the stimulus-responsive nature of the diblock copolymer chains. Moreover, the dye label concentration was maintained at ≈10 μmol m^{-3} during the FCS experiments by diluting the labeled copolymer with an appropriate amount of unlabeled copolymer. Experiments investigating the thermoresponsive behavior of these rhodamine-labeled PGMA-PHPMA diblock copolymer nanoparticles were performed at pH 3.9; the copolymer was freeze-dried after its synthesis and then reconstituted using ice-cold water at this initial pH.[37]

All FCS data were acquired using an inverted LSM510 Meta confocal microscope equipped with a ConFocor2 FCS module. The setup was calibrated using free RhB dye in order to allow optimization of the pinhole dimensions, placement, and filters. RhB is a widely used fluorescent probe and has a diffusion coefficient of

sulfanylpentanoic acid (PETTC) as a CTA (Figure 2).[27] This near-uniform water-soluble macro-CTA was then chain-extended via RAFT aqueous dispersion copolymerization of HPMA and

$4.2 \pm 0.3 \times 10^{-10}$ m^2 s^{-1} at 22.5 °C in water.[38] Thus, measurement of the rate of diffusion of free RhB dye allowed the observation volume to be determined.

Characterization of Diblock Copolymer Order–Order Transitions in Semidilute Aqueous Solution Using Fluorescence . . .

Macromolecular
Rapid Communications

www.mrc-journal.de

A Linkam FTIR600 stage equipped with a T20 system controller was used to control temperature during FCS measurements. The sample was placed in an Ibidi® μ-Dish[35 mm, high] imaging dish. The temperature was lowered from 22 °C to the desired temperature for observation. After allowing 5 min for thermal equilibrium at each temperature, a series of FCS measurements were made before returning to 22 °C.

For studies of the pH-dependent behavior of PGMA-PHPMA diblock copolymer nanoparticles, addition of a buffer solution was deemed inappropriate, as this would alter the concentration of the dye label. Instead, the copolymer was freeze-dried overnight from its aqueous solution. A small quantity was placed in each well of a Nunc Lab-Tek II 8-chamber slide. The copolymer was then dispersed in an ice-cold buffer solution at a well-defined pH so that the chains adopted their equilibrium copolymer morphology (either worms or spheres) at each pH. All pH-dependent experiments were performed at 22 °C.

FCS data are acquired in the form of an autocorrelation function, $G(\tau)$, given by

$$G(t) = G_\infty + \frac{G_3(\tau)}{n\left(1 + \frac{\tau}{\tau_D}\right)\sqrt{1 + \frac{\tau}{\tau_D S^2}}} \qquad (1)$$

where G_∞ describes the behavior at infinite time (for data such as these that fluctuate around a mean value, $G_\infty = 1$), $G_3(\tau)$ is the autocorrelation of the triplet state decay, n is the number of dye labels within the confocal volume, τ_D describes the characteristic diffusion time of molecules within the confocal volume, and S is a calibration parameter which depends on the width of the confocal volume (400–600 nm). The resulting curve describes the persistence of the fluorescence intensity over a given time period, and fitting is used to determine the physical parameters of the system.

Each measurement was made for 6 s and repeated 150 times. Measurements with average count rates less than 1 kHz were discarded.

To confirm conjugation of the RhB dye label to the PGMA-PHPMA copolymer chains, preliminary FCS measurements were conducted without changing either temperature or pH. If free RhB were present, its contribution to the rate of diffusion would be detected. If a contribution from free RhB was observed, the sample was removed and purification was repeated until the only contribution to the correlation curve was from covalently bound RhB labels. All data presented herein were obtained for rigorously purified samples.

3. Results and Discussion

Rheological experiments performed on the HOOC-PGMA$_{43}$-block-P(HPMA$_{119}$-co-GlyMA$_1$) diblock copolymer worm gel revealed their critical gelation temperature (CGT) to be 13 °C (see Figure S3 in the Supporting Information). For Stokes–Einstein diffusion, a higher temperature leads to a corresponding increase in the diffusion coefficient for a

given molecular or colloidal species. However, in the case of the HOOC-PGMA$_{43}$-block-P(HPMA$_{119}$-co-GlyMA$_1$) nanoparticles, this relationship breaks down as the relatively massive worms are converted into much smaller spheres. The characteristic temperature at which this transition occurs is the CGT and represents the difference between the rates of diffusion of spheres and worms, respectively, in aqueous dispersion. Worms and spheres were never observed in coexistence at any temperature or pH examined in this study. This suggests a relatively rapid transition between these two copolymer morphologies (within a timescale of seconds).

The diffusion coefficient was reduced by more than a factor of four with increasing temperature; see Figure 3. Furthermore, the FCS data illustrate the sharpness of this thermal transition, with the change in diffusion coefficient occurring over less than 2 °C. The Stokes–Einstein equation was used to calculate hydrodynamic radii,

$$r_H = \frac{k_B T}{6\pi\rho D}. \qquad (2)$$

The corresponding hydrodynamic radii are 15 ± 2 nm for spheres at 11 °C and 55 ± 14 nm for worms at 15 °C. Here, T is the absolute temperature, i.e., 284 and 288 K, respectively; ρ is the dynamic viscosity of water, or 1.3 mPa s at 11 °C and 1.1 mPa s at 15 °C;[39] D is the diffusion coefficient calculated from curve-fitting; and k_B is the Boltzmann constant. The worms are highly anisotropic, but the Stokes–Einstein equation is strictly only valid for spherical particles in dilute solutions of low-Reynolds number; hence sphere-equivalent diameters are reported. Using Equation (1), the dye concentration was determined to be 16 ± 2 μmol m^{-3} for the spheres and 26 ± 3 μmol m^{-3}
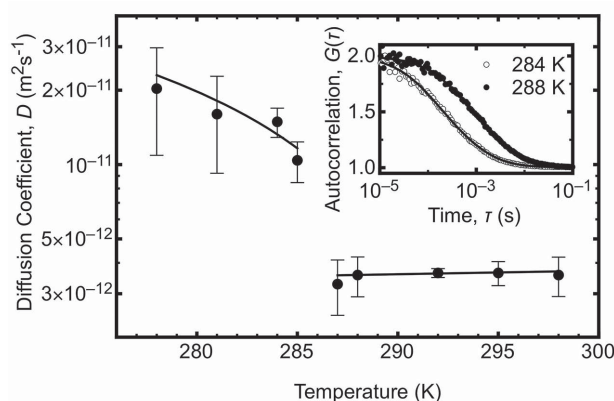

Figure 3. Diffusion coefficients determined for PGMA$_{43}$-block-P(HPMA$_{119}$-co-GlyMA$_1$) nanoparticles as a function of temperature, illustrating the worm-to-sphere transition as the temperature is lowered below 13 °C (286 K). The inset shows selected FCS data collected either side of the transition. The solid lines represent fits to Equation (1).
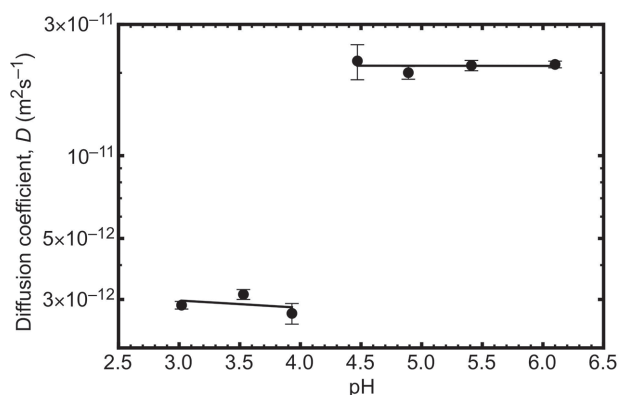
Figure 4. Diffusion coefficients determined at 22 °C for PGMA$_{43}$-*block*-P(HPMA$_{119}$-*co*-GlyMA$_1$) nanoparticles as a function of pH, illustrating the worm-to-sphere transition as the solution pH is gradually increased from pH 3.0 to pH 6.2.

for the worms. The difference between the two results is likely to be because dyes located in the same micelle are correlated. Visible absorption spectroscopy analysis of the dissolved copolymer chains indicated a rhodamine dye label concentration of 7 µmol m^{-3}.

In a control experiment, the hydrodynamic radius of the HOOC-PGMA$_{43}$-*block*-P(HPMA$_{119}$-*co*-GlyMA$_1$) diblock copolymer in methanol was measured to be 1.01 ± 0.04 nm, suggesting molecular dissolution of the copolymer chains under these conditions. This is consistent with small-angle X-ray scattering (SAXS) studies recently reported for closely related PGMA$_{57}$-*block*-PHPMA$_{140}$ in methanol.[37] Thus, the steady increase in diffusion coefficient that is observed in Figure 3 below the worm-to-sphere transition is consistent with the partial dissociation of the spheres to form near-molecularly dissolved copolymer chains at sufficiently low temperatures.[37] However, the temperature at which this order–disorder transition occurs is not reached in the current study, with the smallest radius observed being 8 ± 4 nm at 5 °C.

The pH-dependent behavior of the diffusion coefficient of the HOOC-PGMA$_{43}$-*block*-P(HPMA$_{119}$-*co*-GlyMA$_1$) nanoparticles is shown in Figure 4. As the solution pH is increased above pH 4.0, the diffusion coefficient increases by a factor of approximately eight. Again, this indicates a worm-to-sphere transition, in this case caused by a rather subtle end-group ionization effect.[27] The critical pH observed for this worm-to-sphere transition (pH 4.2) is in good agreement with that indicated for closely related HOOC-PGMA$_{56}$-*block*-PHPMA$_{155}$ diblock copolymer nanoparticles by rheology measurements[27] and also dynamic light scattering (DLS) studies of the HOOC-PGMA$_{43}$-*block*-P(HPMA$_{119}$-*co*-GlyMA$_1$) nanoparticles (see Figure S4 in the Supporting Information). When considering the self-consistency of the observed thermoresponsive behavior, it should be noted that the solution pH for the latter

formulation was pH 3.9. Thus the diffusion coefficients are self-consistent when comparing identical conditions.

4. Conclusions

In summary, FCS has been used to characterize two worm-to-sphere transitions for HOOC-PGMA$_{43}$-*block*-P(HPMA$_{119}$-*co*-GlyMA$_1$) nanoparticles that can be induced by varying either the solution temperature or pH. The absence of secondary components at intermediate temperatures or pH values suggests that this order–order transition is relatively fast, as the two phases do not coexist on the time scale of a single FCS measurement. It is emphasized that FCS provides additional information compared to DLS, since the former technique enables such phase transitions to be monitored over the same semidilute concentration range as that employed for rheology studies, rather than merely in highly dilute solution. This is important, because the worm-to-sphere transition is reversible when conducted at copolymer concentrations of 5%–10% solids, but becomes irreversible at 0.1%–1.0% solids (i.e., in the DLS regime).

Supporting Information

Supporting Information is available from the Wiley Online Library or from the author.

[1] B. Jeong, Y. H. Bae, D. S. Lee, S. W. Kim, *Nature* **1997**, *388*, 860.
[2] C. Tsitsilianis, *Soft Matter* **2010**, *6*, 2372.
[3] C. Li, Y. Tang, S. P. Armes, C. J. Morris, S. F. Rose, A. W. Lloyd, A. L. Lewis, *Biomacromolecules* **2005**, *6*, 994.
[4] J. Madsen, S. P. Armes, A. L. Lewis, *Macromolecules* **2006**, *39*, 7455.
[5] A. P. Blum, J. K. Kammeyer, A. M. Rush, C. E. Callmann, M. E. Hahn, N. C. Gianneschi, *J. Am. Chem. Soc.* **2015**, *137*, 2140.
[6] C. de las Heras Alarcón, S. Pennadam, C. Alexander, *Chem. Soc. Rev.* **2005**, *34*, 276.
[7] Y. Ma, Y. Tang, N. C. Billingham, S. P. Armes, A. L. Lewis, *Biomacromolecules* **2003**, *4*, 864.

Characterization of Diblock Copolymer Order–Order Transitions in Semidilute Aqueous Solution Using Fluorescence . . .

Macromolecular
Rapid Communications

www.mrc-journal.de

[8] D. Roy, J. N. Cambre, B. S. Sumerlin, *Prog. Polym. Sci.* **2010**, *35*, 278.

[9] A. Blanazs, R. Verber, O. O. Mykhaylyk, A. J. Ryan, J. Z. Heath, C. W. I. Douglas, S. P. Armes, *J. Am. Chem. Soc.* **2012**, *134*, 9741.

[10] Z. An, Q. Shi, W. Tang, C.-K. Tsung, C. J. Hawker, G. D. Stucky, *J. Am. Chem. Soc.* **2007**, *129*, 14493.

[11] A. Blanazs, J. Madsen, G. Battaglia, A. J. Ryan, S. P. Armes, *J. Am. Chem. Soc.* **2011**, *133*, 16581.

[12] Y. Li, S. P. Armes, *Angew. Chem. Int. Ed.* **2010**, *49*, 4042.

[13] J. Rieger, C. Grazon, B. Charleux, D. Alaimo, C. Jérôme, *J. Polym. Sci. A: Polym. Chem.* **2009**, *47*, 2373.

[14] J. Chiefari, Y. K. Chong, F. Ercole, J. Krstina, J. Jeffery, T. P. T. Le, R. T. A. Mayadunne, G. F. Meijs, C. L. Moad, G. Moad, E. Rizzardo, S. H. Thang, *Macromolecules* **1998**, *31*, 5559.

[15] G. Moad, E. Rizzardo, S. H. Thang, *Aust. J. Chem.* **2012**, *65*, 985.

[16] S. Perrier, P. Takolpuckdee, *J. Polym. Sci. A: Polym. Chem.* **2005**, *43*, 5347.

[17] C. A. Figg, A. Simula, K. A. Gebre, B. S. Tucker, D. M. Haddleton, B. S. Sumerlin, *Chem. Sci.* **2015**, *6*, 1230.

[18] L. Houillot, C. Bui, M. Save, B. Charleux, C. Farcet, C. Moire, J.-A. Raust, I. Rodriguez, *Macromolecules* **2007**, *40*, 6500.

[19] G. Liu, Q. Qiu, Z. An, *Polym. Chem.* **2012**, *3*, 504.

[20] G. Liu, Q. Qiu, W. Shen, Z. An, *Macromolecules* **2011**, *44*, 5237.

[21] Y. Pei, N. C. Dharsana, J. A. van Hensbergen, R. P. Burford, P. J. Roth, A. B. Lowe, *Soft Matter* **2014**, *10*, 5787.

[22] Y. Pei, A. B. Lowe, *Polym. Chem.* **2014**, *5*, 2342.

[23] Y. Pei, L. Thurairajah, O. R. Sugita, A. B. Lowe, *Macromolecules* **2015**, *48*, 236.

[24] N. Suchao-in, S. Chirachanchai, S. Perrier, *Polymer* **2009**, *50*, 4151.

[25] W.-M. Wan, C.-Y. Pan, *Macromolecules* **2010**, *43*, 2672.

[26] W. Zhao, G. Gody, S. Dong, P. B. Zetterlund, S. Perrier, *Polym. Chem.* **2014**, *5*, 6990.

[27] J. R. Lovett, N. J. Warren, L. P. D. Ratcliffe, M. K. Kocik, S. P. Armes, *Angew. Chem. Int. Ed.* **2015**, *54*, 1279.

[28] E. L. Elson, D. Magde, *Biopolymers* **1974**, *13*, 1.

[29] K. Koynov, H.-J. Butt, *Curr. Opin. Colloid Interface Sci.* **2012**, *17*, 377.

[30] O. Krichevsky, G. Bonnet, *Rep. Prog. Phys.* **2002**, *65*, 251.

[31] C. Lellig, J. Wagner, R. Hempelmann, S. Keller, D. Lumma, W. Härtl, *J. Chem. Phys.* **2004**, *121*, 7022.

[32] U. Zettl, S. T. Hoffmann, F. Koberling, G. Krausch, J. Enderlein, L. Harnau, M. Ballauff, *Macromolecules* **2009**, *42*, 9537.

[33] L. Edman, Ü. Mets, R. Rigler, *Proc. Natl Acad. Sci. USA* **1996**, *93*, 6710.

[34] F. Wang, Y. Shi, S. Luo, Y. Chen, J. Zhao, *Macromolecules* **2012**, *45*, 9196.

[35] D. Schaeffel, A. Kreyes, Y. Zhao, K. Landfester, H.-J. Butt, D. Crespy, K. Koynov, *ACS Macro Lett.* **2014**, *3*, 428.

[36] L. Yu, M. Tan, B. Ho, J. L. Ding, T. Wohland, *Anal. Chim. Acta* **2006**, *556*, 216.

[37] M. K. Kocik, O. O. Mykhaylyk, S. P. Armes, *Soft Matter* **2014**, *10*, 3984.

[38] P.-O. Gendron, F. Avaltroni, K. J. Wilkinson, *J. Fluorescence* **2008**, *18*, 1093.

[39] J. Kestin, M. Sokolov, W. A. Wakeham, *J. Phys. Chem. Ref. Data* **1978**, *7*, 941.